Biochemistry

Subscriber access provided by UNIVERSITY OF ADELAIDE LIBRARIES

Article

"Transition state analogue inhibitors of 5'-deoxyadenosine/5'-methylthioadenosine nucleosidase from Mycobacterium tuberculosis"

Hilda A. Namanja-Magliano, Gary B. Evans, Rajesh Harijan, Peter C. Tyler, and Vern L. Schramm

Biochemistry, **Just Accepted Manuscript** • DOI: 10.1021/acs.biochem.7b00576 • Publication Date (Web): 24 Aug 2017

Downloaded from http://pubs.acs.org on August 31, 2017

Just Accepted

"Just Accepted" manuscripts have been peer-reviewed and accepted for publication. They are posted online prior to technical editing, formatting for publication and author proofing. The American Chemical Society provides "Just Accepted" as a free service to the research community to expedite the dissemination of scientific material as soon as possible after acceptance. "Just Accepted" manuscripts appear in full in PDF format accompanied by an HTML abstract. "Just Accepted" manuscripts have been fully peer reviewed, but should not be considered the official version of record. They are accessible to all readers and citable by the Digital Object Identifier (DOI®). "Just Accepted" is an optional service offered to authors. Therefore, the "Just Accepted" Web site may not include all articles that will be published in the journal. After a manuscript is technically edited and formatted, it will be removed from the "Just Accepted" Web site and published as an ASAP article. Note that technical editing may introduce minor changes to the manuscript text and/or graphics which could affect content, and all legal disclaimers and ethical guidelines that apply to the journal pertain. ACS cannot be held responsible for errors or consequences arising from the use of information contained in these "Just Accepted" manuscripts.

ACS Publications

Biochemistry is published by the American Chemical Society. 1155 Sixteenth Street N.W., Washington, DC 20036

Published by American Chemical Society. Copyright © American Chemical Society. However, no copyright claim is made to original U.S. Government works, or works produced by employees of any Commonwealth realm Crown government in the course of their duties.

Transition state analogue inhibitors of 5'-deoxyadenosine / 5'-methylthioadenosine nucleosidase from *Mycobacterium tuberculosis*

Hilda A. Namanja-Magliano[1], Gary B. Evans[2,3], Rajesh K. Harijan[1], Peter C. Tyler [2], and Vern L. Schramm [1,*]

[1]Department of Biochemistry, Albert Einstein College of Medicine, 1300 Morris Park Avenue, Bronx, New York 10461, United States

[2]The Ferrier Research Institute, Victoria University of Wellington , Lower Hutt, Wellington 5040, New Zealand

[3]The Maurice Wilkins Centre for Molecular Biodiscovery, The University of Auckland, New Zealand

KEYWORDS

Rv0091, MTAN, ribocation analogues, Immucillins, DADMe-Immucillins

ABSTRACT

Mycobacterium tuberculosis 5'-deoxyadenosine/5'-methylthioadenosine nucleosidase (Rv0091) catalyzes the *N*-riboside hydrolysis of its substrates 5'-methylthioadenosine (MTA) and 5′-deoxyadenosine (5'-dAdo). 5'-dAdo is the preferred substrate, a product of radical SAM-dependent enzyme reactions. Rv0091 is characterized by a ribocation-like transition state, with low N-ribosidic bond order, an *N*7 protonated adenine leaving group and an activated but weakly bonded water nucleophile. DADMe-Immucillins incorporating 5'-substituents of the substrates 5'-dAdo and MTA were synthesized and characterized as inhibitors of Rv0091. 5'-Deoxy-DADMe Immucillin-A was the most potent among the 5'-dAdo transition state analogs with a dissociation constant of 640 pM. Among the 5'-thio substituents, hexylthio-DADMe-Immucillin-A was the best inhibitor at 87 pM. The specificity of Rv0091 for the Immucillin transition state analogues differs from other bacterial homologues because of an altered hydrophobic tunnel accepting the 5'-substituents. Inhibitors of Rv0091 had weak cell growth effects on *Mycobacterium tuberculosis* or *Mycobacterium smegmatis*, but were lethal towards *Helicobacter pylori*, where the 5'-methylthioadenosine nucleosidase is essential in menaquinone biosynthesis. We propose that Rv0091 plays a role in 5'-deoxyadenosine recycling, but is not essential for growth in these *Mycobacteria*.

INTRODUCTION

5'-Methylthioadenosine/*S*-adenosylhomocysteine nucleosidases (MTANs) are absent in human metabolism, however in bacteria, they are involved in pathways related to *S*-adenosylmethionine (SAM) recycling, quorum sensing, methylation, menaquinone and polyamine biosynthesis.[1-3] The MTANs catalyze *N*-ribosidic bond hydrolysis of 5'-methylthioadenosine (MTA), *S*-adenosylhomocysteine (SAH), and 5'-deoxyadenosine (5'-dAdo). *Mycobacterium tuberculosis* (*M. tuberculosis*) Rv0091 was originally annotated as MTAN, however recent studies demonstrates that it functions primarily as a 5'-dAdo nucleosidase.[4] 5'-dAdo is generated together with methionine as products of radical SAM-dependent enzyme reactions (Scheme. 1).[5] The *M. tuberculosis* genome encodes 21 open reading frames annotated as radical SAM enzymes based on the sequence analysis identifying an iron-sulfur CX_3CX_2C motif that has been linked to radical SAM function.[6] Accumulation of 5'-dAdo is reported to block the activity of some SAM-related enzymes as a product inhibitor.[3]

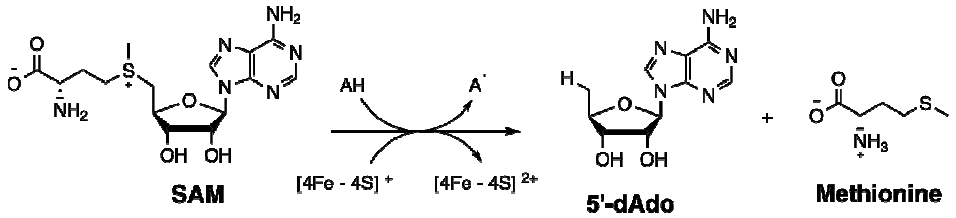

Scheme 1. Reaction catalyzed by radical SAM enzymes for the reductive cleavage of SAM with [4Fe – 4S]$^+$ in the presence of substrate [AH] to give 5'-dAdo and methionine

Tuberculosis (TB) is one of the most difficult bacterial infections as a result of the spread of multidrug resistant strains. TB affects one third of the world population and is resistant to many of the current antibacterial therapies.[7] TB poses a worldwide threat and new antibiotics are needed to treat the causative agent, *M. tuberculosis.* Here we explore the transition state

analogue specificity of Rv0091 MTAN and test several inhibitors against cultured organisms as potential antibacterials.

Transition state analogues capture the geometry and electrostatic features of an enzymatic transition state in chemically stable structures. The analogues have the potential to bind to the enzyme much tighter than the substrate, with an upper limit of the factor equal to the catalytic enhancement imposed by the enzyme, relative to the Michaelis complex.[8-10] A perfect transition state analogue is impossible to design, as the actual transition state structure consists of non-equilibrium bond lengths and charge distributions that cannot be captured in a stable molecule. The Immucillins and DADMe-Immucillins are stable transition state analogues of *N*-ribosyltransferases developed from transition state analysis using kinetic isotope effects (KIEs) and computational chemistry.[11-13] Several bacterial MTANs are inhibited by these compounds with potent dissociation constants (fM – pM range).[14-17]

Previously, the transition state structure of *M. tuberculosis* Rv0091 was analyzed and was found to resemble the DADMe-Immucillins.[4] The DADMe-Immucillins contain a 5'-thio group to mimic the MTAN substrate MTA. A family of the DADMe-Immucillins inhibited Rv0091 with dissociation constants with pM to nM affinity. 5'-dAdo was previously shown to be the preferred substrate of Rv0091, therefore, we anticipated transition state analogues similar to the transition state for 5'-dAdo to have the best affinities. In this study, we incorporate features of 5'-dAdo into transition state analogue design. Inhibition constants are established for several 5'-deoxyalkyl-DADMe-Immucillin-A compounds. Chemical synthesis and inhibition is described for the novel compound 5'-deoxy-DADMe-ImmA (**4**). The 5'-deoxyalkyl- and the 5'-thio containing DADMe-Immucillin-A compounds (MTA and SAH substrate features) displayed dissociation constants in the pM to low nM range. The 5'-deoxyalkyl-DADMe-Immucillin

inhibitors show optimal inhibitory activity with short 5'-substituents, while 5'-thioalkyl-DADMe-Immucillins bind most tightly with longer 5'-substituents. This inhibitory pattern is not found in other bacterial MTANs and is therefore unique to Rv0091. Molecular modeling of inhibitors into the catalytic site of Rv0091 indicates an altered binding mode for 5′-substituents compared to other bacterial MTANs.

Bacterial growth assays show that Rv0091 inhibitors have weak effects on the growth of *M. tuberculosis* and *Mycobacterium smegmatis* (*M. smegmatis*). In contrast, the same inhibitors displayed potent antibacterial activity against *Helicobacter pylori* (*H. pylori*) species. The essential nature of MTAN in menaquinone synthesis for *H. pylori* is well documented.[17 18] Thus, the function of Rv0091 MTAN is not essential for laboratory growth in these *Mycobacteria*.

MATERIALS AND METHODS

General experimental approach for inhibitor synthesis. Compounds **5** – **20** were synthesized as previously described.[17, 19-23] Air sensitive reactions were performed under argon. Organic solutions were dried over anhydrous $MgSO_4$ and the solvents were evaporated under reduced pressure. Anhydrous and chromatography solvents were obtained commercially and used without any further purification. Thin layer chromatography (t.l.c.) was performed on glass or aluminum sheets coated with 60 F254 silica gel. Organic compounds were visualized under uv light or use of a dip of ammonium molybdate (5 wt %) and cerium(IV) sulfate 4 H_2O (0.2 wt %) in aq. H_2SO_4 (2 M), one of I_2 (0.2 %) and KI (7%) in H_2SO_4 (1 M), or 0.1 % ninhydrin in EtOH. Chromatography (flash column) was performed on silica gel (40-63 μm) or on an automated system with a continuous gradient facility. ^{1}H NMR spectra were measured in $CDCl_3$, CD_3OD, DMSO d_6 (internal Me_4Si, δ 0) or methanol-d_4, and ^{13}C NMR spectra in $CDCl_3$ (centre line, δ

77.0), CD_3OD (centre line, δ 49.0),. Assignments of ^1H and ^{13}C resonances were based on 2D (^1H-^1H DQF-COSY, ^1H-^{13}C HSQC, HMBC) and DEPT experiments. Positive electrospray mass spectra were recorded on a Q-TOF Tandem Mass Spectrometer.

(3*S*,4*R*)-*tert*-Butyl-3-(bromomethyl)-4-hydroxypyrrolidine-1-carboxylate (2) synthesis. Methanesulfonyl chloride (0.45 ml., 5.7 mmol) was added dropwise to a stirred solution of *tert*-butyl 3-hydroxy-4-(hydroxymethyl)pyrrolidine-1-carboxylate (**1**) (1.13 g, 5.2 mmol) and 2,6-dimethylpyridine (1.2 mL, 10.3 mmol) in acetone (20 mL) and the mixture left stirring for 24 h. The resulting suspension was filtered to remove salt and then lithium bromide (2.25 g, 25.9 mmol) was added to the filtrate and the mixture refluxed for 3h at which time the reaction was deemed complete. The crude reaction mixture was absorbed onto silica gel (5 g), concentrated *in vacuo* and the resulting residue purified by chromatography (20%=>40%=>100% EA:PE) to afford the title compound **2** (832 mg, 57%) as a syrup. ^1H NMR (500 MHz, $CDCl_3$) δ 4.06 (brs, 1H), 3.67 (brs 2H), 3.47 – 3.36 (m, 2H), 3.28 – 3.18 (m, 2H), 2.50 (brs, 1H), 1.46 (s, 9H). ^{13}C NMR (125 MHz, $CDCl_3$) δ 154.6, 79.9, (73.3, 72.5), (52.6, 52.3), (48.8, 48.3), (48.2, 47.6), 32.6, 28.5. HRMS (ESI) m/z calcd for $C_{10}H_{18}NO_3BrNa^+$ 302.0368, obsd 302.0364.

(3*R*,4*S*)-4-Methylpyrrolidin-3-ol (3) synthesis. A mixture of **2**, triethylamine (1.85 mL, 13.2 mmol), and Perlman's catalyst (150 mg, 1.0 mmol) in ethanol (20 mL) was stirred under an atmosphere of hydrogen for 3h. The crude reaction mixture was then filtered through Celite and concentrated *in vacuo* and the residue dissolved in methanol (2 mL) and conc HCl (2 mL) and concentrated *in vacuo*. The resulting syrup was dissolved in additional conc HCl (2 ml) and concentrated *in vacuo*. The residue was dissolved in MeOH and absorbed onto silica, concentrated *in vacuo* and the resulting solid was purified by chromatography (30% 7*N* NH_3 in MeOH:$CHCl_3$) to afford the title compound **3** (501 mg, 97%) as an oil. ^1H NMR (500 MHz,

$CDCl_3$) δ 4.24 (brs, 1H), 3.65 - 3.55 (m 2H), 3.25 (d, *J* = 15.0 Hz, 1H), 3.08 – 3.04 (m, 1H), 2.39 (brs, 1H), 1.09 (d, *J* = 10.0 Hz, 3H). ^{13}C NMR (125 MHz, $CDCl_3$) δ 75.5, 50.8, 50.2, 39.9, 15.1. HRMS (ESI) m/z calcd for $C_5H_{12}NO$ $[MH]^+$ 102.0919, obsd 102.0914.

(*3R,4S*)-1-[(9-Deazahypoxanthin-9-yl)methyl]-3-hydroxy-4-methylpyrrolidine (4) synthesis. Formaldehyde (0.41 mL 5.4 mmol, 37 mass% aq) was added to a stirred suspension of **3** (500 mg, 4.9 mmol,) and 9-deazaadenine (77 mg 5.4 mmol) in a water (2.5 mL) and ethanol (5 mL) mixture and then left to stir at room temperature for 48 h. The crude reaction mixture was absorbed onto silica, concentrated *in vacuo* and the solid residue purified by silica gel chromatography to afford the title compound **4** (647 mg, 53%) as a solid. ^{1}H NMR (500 MHz, Methanol-d_4) δ 8.18 (s, 1H), 7.49 (s, 1H), 3.87 – 3.74 (m, 2H), 3.37 (s, 1H), 3.05 (dd, *J* = 9.6, 7.7 Hz, 1H), 2.82 (dd, *J* = 10.4, 6.5 Hz, 1H), 2.70 (dd, *J* = 10.4, 4.3 Hz, 1H), 2.17 (dd, *J* = 9.6, 7.9 Hz, 1H), 2.04 (ht, *J* = 7.2, 3.5 Hz, 1H), 1.05 (d, *J* = 6.9 Hz, 3H).. ^{13}C NMR (125 MHz, Methanol-d_4) δ 152.1, 151.0, 147.0, 130.1, 115.1, 112.6, 79.0, 62.1, 61.0, 49.2, 43.0, 17.8. HRMS (ESI) m/z calcd for $C_{12}H_{18}N_4O$ $[MH]^+$ 248.1511, obsd 248.1508.

Expression and purification of 5′-deoxyadenosine/ 5′-methylthioadenosine nucleosidase. Enzyme expression and purification were done as described previously.[4] Briefly, *E. coli* BL21 Star^{TM} (DE3) plysS cell lines were employed for expression. A 25 mL initial culture with LB medium (Gibco) supplemented with ampicillin (100 µg/mL) and chloramphenicol (100 µg/mL) was incubated overnight at 37 °C. The following day, 6 mL of culture was added to 1 L of fresh LB-ampicillin (100 µg/mL) and incubated at 37 °C to an OD_{600} of 0.6 to 0.8. Cells were induced with 0.5 mM isopropyl-D-thiogalactoside (IPTG) (Goldbio) and incubated overnight at 28 °C. Cells were harvested and protein purified by Ni-NTA (Qiagen) chromatography with a 30 to 250 mM imidazole buffer containing 20 mM Tris-HCl pH 7.4 and 300 mM NaCl. Fractions

containing purified protein (greater than 90% by SDS-gel) were pooled, exchanged into 50 mM HEPES, pH 7.4 and 10% glycerol and stored at –80 °C.

Dissociation constants. Dissociation constants (K_i values) of Rv0091 inhibitors were determined as previously described.[24] Briefly, the 5′-dAdo nucleosidase reaction was coupled with 1 unit xanthine oxidase (Sigma-Aldrich) in the presence of 1 mM 5′-dAdo and varying concentrations of inhibitor in 50 mM HEPES, pH 7.4, at 25 °C. Formation of 2,8-dihydroxyadenine was monitored at 305 nm for 2 hours. The reactions were initiated by adding 10 nM of enzyme. The K_i values were obtained from the rates with and without inhibitors (v_i / v_0) that were fitted using the Morrison quadradic equation for tight-binding inhibitors Eq. 1 on GraphPad Prism.[25] The K_M for 5′-dAdo is 10.9 μM, E, I and S are enzyme, inhibitor and substrate concentrations, respectively.[4]

Eq. 1

$$v = v_o\left(1-\left(\left[E_T\right]+\left[I\right]+\left(K_i\left(1+\frac{[S]}{K_M}\right)\right)\right)\right)-\frac{\sqrt{\left(\left[E_T\right]+\left[I\right]+K_i\left(1+\frac{[S]}{K_M}\right)\right)^2-4\left[E_T\right]\left[I\right]}}{2\left[E_T\right]}$$

Antibacterial testing. *Mycobacterium smegmatis* (*M. smegmatis*) strain mc^{2}155 and *M. tuberculosis* mc^{2}6230 (non-pathogenic; pantothenate auxotroph) were cultured in Middlebrook 7H9 liquid media (Difco) to an OD_{600} = 0.6 and plated on Middlebrook 7H10 agar plates as described previously.[26, 27] Bacterial growth inhibition was determined by a drug diffusion method. Test compounds were added to the center of discs and placed on *M. smegmatis* and *M. tuberculosis* inoculated plates and allowed to grow for 96 hours at 37 °C.

Antibacterial activity assay with *H. pylori*. *H. pylori* was grown under microaerophilic conditions (5% O_2, 10% CO_2 and 85% N_2) at 37 °C in brain heart infusion medium (Oxoid) with 10% fetal bovine serum (Gibco) and DENT supplement (Oxoid). HT-DADMe ImmA and tetracycline (Sigma-Aldrich) stocks were made in culture medium and MIC values were determined by adding 50 μL of varied drug concentrations in a 96 well plate format at 2X concentration in culture medium. Cultured *H. pylori* (50 μL) was added to the medium with inhibitor. After 72 hours incubation in a microaerophilic conditions at 37 °C, the OD at 600 nm was determined on a SpectraMax plate reader and MIC_{50} values obtained using a non-linear regression curve fit using GraphPad prism.

Homology modeling. An *in silico* model of Rv0091 for structure prediction was performed by the I-TASSER, an online homology platform for automated protein structure prediction without any additional templates.[28] The structural comparisons of the Rv0091 model to MTAN structures with close homology was accomplished with the secondary structure matching (SSM) algorithm in COOT.[29] The superposition of the binding site of Rv0091 was done in comparison to *H. pylori* MTAN (HpMTAN; PDB ID: 4FFS) and *E. coli* MTAN (EcMTAN, PDB ID: 4WKC).

The Rv0091 model was analyzed by molecular docking with AutoDock Vina for binding with the transition state analogues BT-DADMe-ImmA (**13**) and HT-DADMe-ImmA (**14**).[30] Coordinates for BT-DADMe-ImmA were obtained from BT-DADMe-ImmA bound to HpMTAN (PDB ID: 4FFS). Coordinates for HT-DADMe-ImmA (**14**) were generated and optimized using the eLBOW function of the PHENIX system for macromolecular structures.[31] Molecular docking was performed using a grid box of the whole protein. The potential binding site for BT-DADMe-ImmA and HT-DADAMe-ImmA was identified by applying the binding mode of the inhibitors to the Rv0091 model. A second round of docking was done with the

smaller grid (14 x 14 x 14 Å), centered on the binding site. The search completeness was evaluated by the default value E = 8 during docking with AutoDock Vina. The binding site analysis and comparisons were done with the published structures of HpMTAN (4FFS) and EcMTAN (4WKC).[17, 32] The figures were made by using PyMOL (The PyMOL Molecular Graphics System, Version 1.3, Schrödinger, LLC).

RESULTS AND DISCUSSION

DADMe-Immucillin mimics of the 5′-substituent of Rv0091 substrates.

The transition state structure of *M. tuberculosis* Rv0091 revealed a ribocation-like ribose ring with low C1′–N9 bond order, protonation of the adenine leaving group and weak participation of the water nucleophile (Scheme. 2).[4] The 5'-alkylthio-DADMe-Immucillin inhibitors resemble the Rv0091 transition state structure while incorporating features of the MTA substrate. MT-DADMe-ImmA (**11**) incorporates the 5'-methylthio group of MTA and exhibits an inhibition constant of 1.5 ± 0.4 nM (Figure 2, Table 1). Increased hydrophobicity induced by modifying the 5'-substituent group to a 5'-hexylthio (**14**) improved the dissociation constant to 87 ± 12 pM.[4]

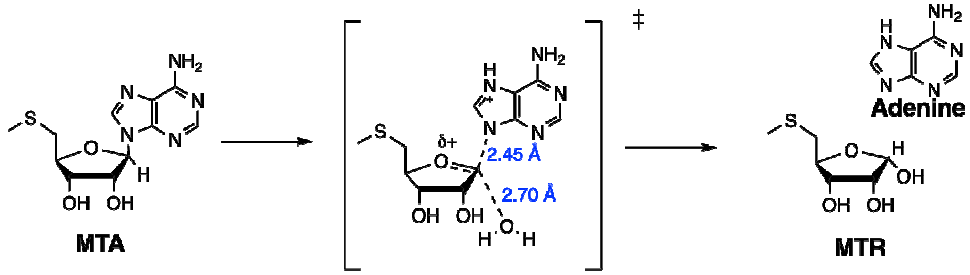

Scheme 2. Reaction and transition state catalyzed by Rv0091 to give adenine and 5-methylthioribose (MTR). The reaction goes through a transition state characterized by a ribocation character, protonation of the adenine leaving group, weak but significant participation of the nucleophillic water and advanced loss of C1'–N9 bond.[4]

Enzyme catalytic theory posits that mimics of the transition state for the most proficient substrate will provide the tightest binding transition state analogue.[8] Values of k_{cat}/K_M for 5'-dAdo, MTA and S-adenosylhomocysteine (SAH) with Rv0091 are reported to be 4.4 x 10^4, 0.6 x 10^4 and 0.006 x 10^4 $M^{-1}s^{-1}$, respectively. Therefore, transition state analogues of 5'-dAdo would be anticipated to have the highest affinity. The transition state structures of MTANs from *E. coli* and *S. pneumonia* showed MTA hydrolysis to be a late dissociative process[14, 15] and that of *N. meningitides* to be an early S_N1 mechanism.[33] Analogues designed to mimic the early dissociative transition state are the immucillins, characterized by a cationic N4′-imino group and a single bond between the ribocation mimic and the 9-deazaapurine mimic of the leaving group. An example is MT-ImmA (**19**; Figure 2). The DADMe-Immucillins incorporate a methylene bridge between the ribocation mimic and the adenine leaving group analogue to more accurately mimic the transition state separation of these two groups. They are often near the fully dissociated C1′–N9 bond distance of 3.0 Å at the transition state.[13, 16] The Rv0091 transition state has a C1′–N9 distance of 2.45 Å and a weakly bonded nucleophillic water, making it intermediate between the early and late N-ribosyltransferase transition states.[4] The geometric preference for early or late transition state mimics was tested with the MTA transition state mimics, MT-ImmA (**19**) and MT-DADMe-ImmA (**11**). The K_i values were 85 nM for (**19**) and 1.5 nM for (**11**), demonstrating the DADMe-immucillin analogues to better mimic the Rv0091 transition state, consistent with the transition state analysis.[4] Here we further explore the DADMe-ImmA analogues but extended their structural features to 5′-dAdo, the preferred substrate.

The catalytic activity of Rv0091 with 5′-dAdo as a substrate is relatively inefficient. Like many enzymes from *M. tuberculosis*, it displays a relatively low catalytic efficiency (k_{cat}/K_M) of

4.4 x 10^4 $M^{-1}s^{-1}$, however this is 7-fold better than for MTA and 730-fold better than for SAH. 5′-Alkylthio-DADMe-Immucillin-A inhibitors mimic the MTA substrate at the transition state and gave K_i constants in the pM to low nM range.[4] Transition state analogues of the 5′-dAdo substrate were obtained by the synthesis of 5′-deoxy-DADMe-ImmA (**4**) and its analogues (Scheme 3). The most similar analogue of the 5′-dAdo transition state (**4)** was a potent inhibitor with a dissociation constant of 0.64 nM (Figure. 1).

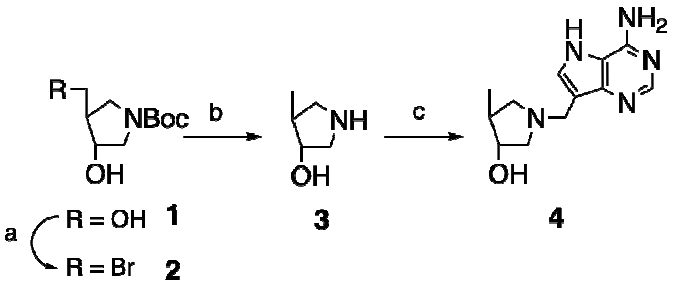

Scheme 3. Synthesis of 5′-deoxy-DADMe ImmucillinA (4). Reagents: (a) (i) MsCl, 2,6-dimethylpyridine, acetone, room temp. (ii) NaBr, 57% for 2 steps; (b) (i) $Pd(OH)_2$, H_2 (g), EtOH, room temp. (ii) cHCl, room temp. 97% yield for two steps. (c) 9-Deazaadenine, 37% aq. formaldehyde, H_2O, EtOH, room temperature 53% yield.

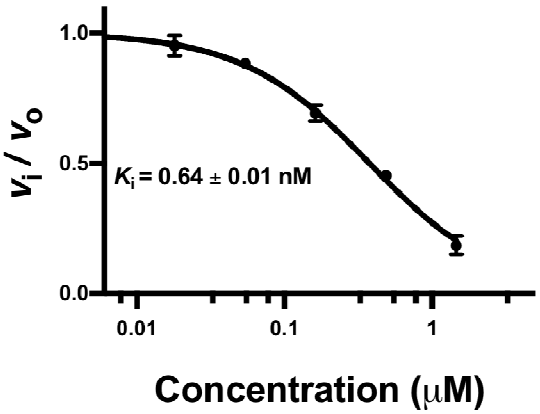

Figure 1. Inhibition of Rv0091 by 5′-deoxy-DADMe-ImmucillinA (4). The reaction rate and inhibition were monitored at 305 nm for the conversion of 5′-dAdo to 2,8-dihydroxyadenine in a reaction coupled to xanthine oxidase as described in the methods. The *K*i value was calculated from the fit to the Morrison equation for tight binding inhibitors.[25] The excess substrate (1.0 mM) relative to its K_m value of 10.9 μM alters the apparent K_i by a factor of 93 for this competitive inhibitor. The true K_i of 0.64 nM is shown.

Crystal structures of *S. enterica*[34] and *H. pylori*[17] MTANs contain hydrophobic tunnels from the 5′-position of bound nucleosides, reaching to the solvent. This structure can accommodate a variety of hydrophobic 5′-substituents. We explored increasing hydrophobicity at the 5′-substituent position, as previously described 5′-thio-DADMe-ImmA analogues (**11-15**) showed favorable binding properties for this change. This is also the case for the 5′-thio-DADMe-ImmA analogues with Rv0091 MTAN. For example, HT-DADMe-ImmA (**14**) bound 17 times tighter than MT-DADMe-ImmA (**11**) (Table 1).[4] However, the hydrophobicity of the 5′-alkyl substituent did not result in improved inhibitor potency for Rv0091 (Figure 2, Table 1). The more hydrophobic 5'-substituent compounds (**5**, **7** and **8)** had slightly weaker inhibition constants relative to the shorter 5'-substituted **4**. Compound **9** containing the longest, but hydrophilic, substituent (PEG) was the weakest inhibitor, at greater than 300 nM K_i. In comparison, **15** which contains a 5'-thio PEG substituent had better potency of 8.2 ± 0.3 nM. These results suggest that the 5'-binding site of Rv0091 is unlike other MTANs in that it prefers 5'-alkyl substituents over 5'-thio if the 5′-substituent is short. When the substituent is longer, the 5'-thio substituents are preferred.

Preference of (3*R*,4*S*)-stereochemistry in the DADMe-Immucillin inhibitors.

The stereochemistry of the 3-hydroxy-4-alkylpyrrolidine moiety on inhibitor potency was explored. The trans-racemate compound **5** was compared to the cis-racemate **6** and was shown to be 13-fold better in potency, demonstrating that the trans stereochemistry is preferred at the 3-hydroxy-4-alkylpyrrolidine position. To evaluate the preference of (3R, 4S) in comparison to (3S, 4R) stereochemistries, the enantiopure (3*R*,4*S*)-MT-DADMe-ImmA (**11**) was compared to the enantiomer (3*S*,4*R*)-MT-DADMe-ImmA (**20**). **11** inhibits Rv0091 with good potency of 1.5 nM while compound **20** had no activity at concentrations to 400 μM. This observation is

consistent with previous findings where (3*R*,4*S*) inhibitors displayed better potencies than their enantiomeric counterparts towards other MTAN nucleosidases including that from *E. coli*.[34]

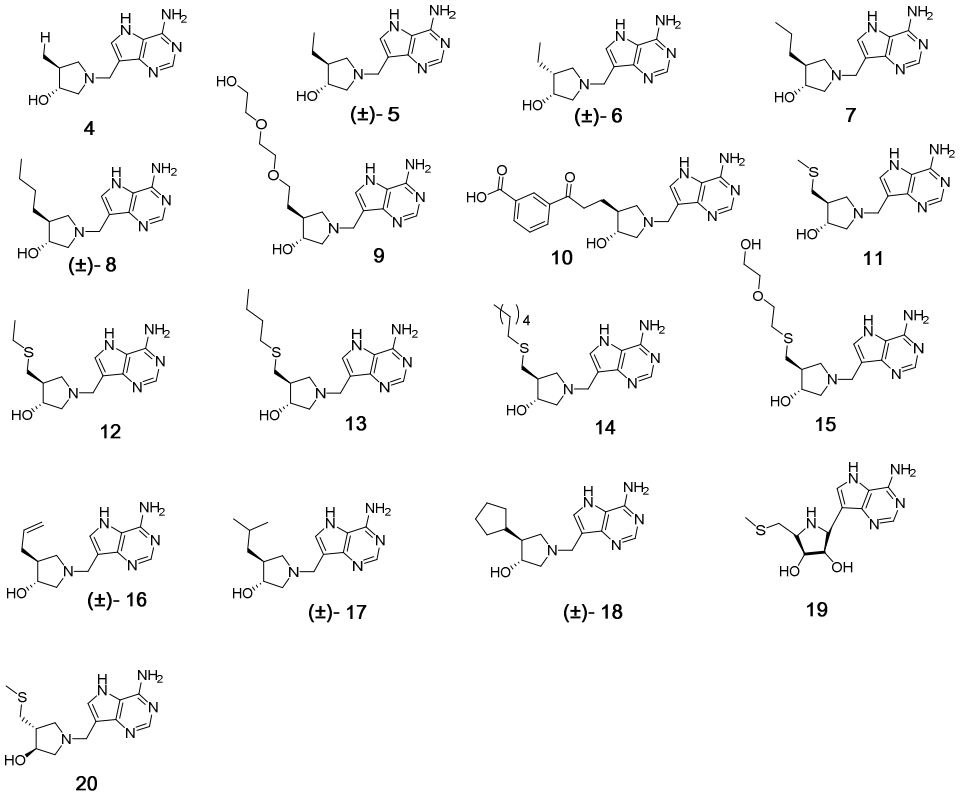

Figure 2. DADMe-Immucillin and Immucillin-based inhibitors of Rv0091. 4,7,9-15, 19 and 20 are enantiopure compounds ; 5, 6, 8, 16 – 18 are racemic mixtures at 3-hydroxy-4-alkylpyrrolidine. Abbreviated names for some of these compounds are provided in the text.

Table 1. Inhibition of Rv0091 with DADMe Immucillin analogues.

Compound	K_i (nM)[a]	Compound	K_i (nM)[a]
4	0.64 ± 0.01	**13**	1.3 ± 0.1[4]
5	1.5 ± 0.1	**14**	0.087 ± 0.012[4]
6	18.9 ± 1.1	**15**	8.2 ± 0.3
7	0.74 ± 0.05	**16**	6.7 ± 0.3
8	1.64 ± 0.20	**17**	2.8 ± 0.2
9	>300	**18**	13.5 ± 1.2
10	5.0 ± 1.1	**19**	85 ± 11[4]
11	1.5 ± 0.4[4]	**20**	NI[b]
12	13.9 ± 2.4		

[a]Dissociation constants are obtained from the xanthine oxidase coupled assay at 25 ºC. The K_i value was calculated by using Equation 1 for analysis of tight binding inhibitors.[25] NI = Not Inhbitor up pt 400 μM.

The affinities of these transition state analogues for Rv0091 (87 pM for the best compound) and other bacterial MTANs, such as *E. coli* MTAN (fM range for best compounds)[20, 35], establishes a reduced affinity for Rv0091. This difference can be attributed to relative catalytic efficiencies of the *E. coli* and *M. tuberculosis* enzymes. Wolfenden postulated that the binding of transition state analogues is associated with enzyme catalytic efficiency.[9, 10] *E. coli* MTAN has a high catalytic efficiency of 4.7 x 10^7 $M^{-1}s^{-1}$ for MTA, approximately 1000-fold more efficient than Rv0091 for 5'-dAdo.[4] The *E. coli* MTAN is also more efficient for 5′-dAdo than is Rv0091 even though it is not a preferred substrate. Consequently, transition state analogues mimicking both MTA and 5′-dAdo substrate are known to bind tighter for the *E. coli* enzyme by several orders of magnitude. This binding is also consistent with previous observations for the inhibitor profiles of the slow *S. pneumonia* MTAN (SpMTAN).[36]

Molecular modeling and putative binding site residues identification

The crystal structure of Rv0091 from *Mycobacterium tuberculosis* is not available. The binding interactions of active site residues for Rv0091 were probed by docking the transition state analogue inhibitors BT-DADMe-ImmA and HT-DADMe-ImmA to explain the difference in 5'-substituent interactions from the specificity known for *H. pylori* and *E. coli* MTANs. The *in silico* model of Rv0091 was generated by I-TESSER server (Figure S1). The best structural model of Rv0091 was obtained with the C-score of 0.43 (ideal C-score is between -5 and 2; a score of 0.43 is an excellent match) and a TM score of 0.77 ± 0.10. The model has a similar structural fold as seen in other MTANs with the exception of an extended loop (from residues Leu148 to Pro162) unique to Rv0091 (Figure S1, S2). Rv0091 shares 29 and 32% sequence identity with *H. pylori* and *E. coli* MTANs, respectively (Figure S2). Comparison of the Rv0091

model with *H. pylori* and *E. coli* MTANs gave RSMD values between 0.96 to 1.03 Å without and with the Rv0091 external loop, respectively.

Crystal structures of *H. pylori* and *E. coli* MTAN in complex with BT-DADMe-ImmA are known.[24, 32] Autodoc-Vina and the *H. pylori* structure with BT-DADMe-ImmA (4FFS) was used for the *in silico* docking of BT-DADMe-ImmH and HT-DADMe-ImmH. The best fit of the interactions between inhibitor and Rv0091 was selected from the top-ranked cluster by binding affinities. Active site superimposition of BT-DADMe-ImmA bound to HpMTAN and EcMTAN with Rv0091 modeled with both BT-DADMe-ImmA and HT-DADMe-ImmA shows the pyrrolidine and deazaadenine inhibitor groups to bind in the same orientation in all the MTANs (Figure 3 and S3). The catalytic site geometry of 5'-alkylthio inhibitor groups differ considerably for Rv0091. The active site tunnel residue Ile52 (in HpMTAN) and Ile50 (at the same position in EcMTAN) has non-polar interactions with the 5'-alkylthio group of the BT-DADMe-ImmA. This interaction is disrupted by the larger Met52 residue in this position in Rv0091 MTAN. The side chain of the Met52 creates a steric clash with 5'-alkylthio group of the inhibitors to displace it relative to its geometry in EcMTAN and HpMTAN (Figure 3).

Inhibitors modeled into Rv0091 show the 3'-hydroxyl group to be hydrogen bonded with Glu197. The N1 and N3 of the 9-deazaadenine ring have hydrogen bonding interactions with the backbone nitrogen of Leu176 and Glu195, respectively. The N6 amino and N7 of the inhibitors form hydrogen bond interactions with both the peptide bond NH of Leu176 and with side chain hydroxyl group of Asp220 (Figure 3 and S3). These groups are conserved between Rv0091, HpMTAN and EcMTAN, supporting the major divergence of Rv0091 being related to the hydrophobic region in the catalytic site that accommodates the 5'-alkylthio groups. The dissociation constant for BT-DADMe-ImmA is 1.3 nM, which is 15 times weaker binding than

HT-DADMe-ImmA (K_d = 87 pM). HT-DADMe-ImmA has two additional carbons at the 5'-alkylthio group that make additional hydrophobic contacts with the enzyme and contributes to the higher affinity of HT-DADMe-ImmA. From the model, the butylthio group of BT-DADMe-ImmA predicts van der Waals interacts with eight amino acids, Ile11, Met52, Met 196, Pro119, Tyr113, Val104, Tyr175 and Phe230. These plus two additional contacts with Glu108 and Val105 are predicted for the hexylthio group of HT-DADMe-ImmA, consistent with its tighter binding.

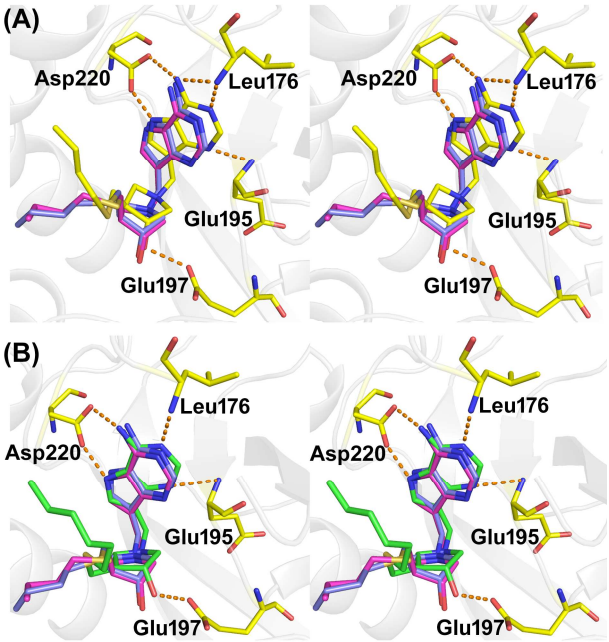

Figure 3. Stereo-view superimposition of the active sites of *H. pylori* and *E. coli* MTAN in complex with BT-DADMe-ImmA compared with Rv0091. The interactions of binding site residues of Rv0091 modeled with BT-DADMe-ImmA (yellow, panel-A) and with HT-DADMe-ImmA (green, panel-B) are highlighted. The BT-DADMe-ImmA of *H. pylori* and *E. coli* are shown in blue and pink, respectively.

Antibiotic activity against *Mycobacterium* species and *H. pylori.*

The antibacterial activity of DADMe-Immucillin compounds was investigated in a disc-diffusion assay against *M. tuberculosis* mc^{2}6230 and *M. smegmatis* mc^{2}155 strains.[37] HT-DADMe-ImmA (**14**) is the most potent inhibitor towards Rv0091 and displayed a small zone of

clearance at 1000 μg/mL in both *Mycobacterium* species (Figure. 4A and 4B). Kanamycin as an antibiotic control displayed large zones of clearance at 100 μg/mL. Other DADMe-Immucillin compounds showed similar results to HT-DADMe-ImmA (**14**) indicating that the function of Rv0091 is not essential for *Mycobacteria* growth. This finding is in agreement with previous gene deletion experiments in *M. tuberculosis*, where Rv0091 was found to be non-essential for growth or for infection.[38, 39] Unlike *Mycobacteria,* MTAN has an essential function in menaquinone synthesis in *H. pylori*.[17] We tested HT-DADMe-ImmA (**14**) in a cultured cell assay using *H. pylori* with tetracycline as a control. HT-DADMe-ImmA (**14**) exhibited antibacterial activity against *H. pylori* with an IC_{50} of 13.0 ± 1.8 ng/mL (equivalent to 35 ± 5 nM), which is six times more potent than tetracycline as an antibiotic (Figure 4C).

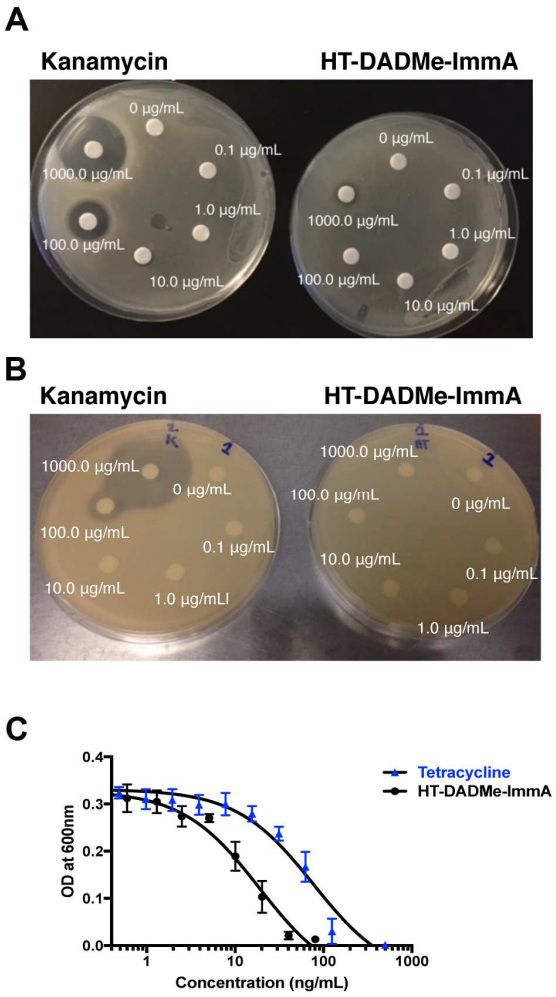

Figure 4. Antibacterial activity. Transition state analogue HT-DADMe-ImmA (**14**) and antibiotic control were tested for growth inhibition against (**A**) *M. smegmatis* mc^{2}155 and (**B**) *M. tuberculosis* mc^{2}6230 in a disc diffusion assay by growth for 96 hours 37 °C on agar plates. (**C**) Inhibition of *Helicobacter pylori* (J99) growth at 37 °C in liquid culture by HT-DADMe-ImmA (**14**) and by tetracycline. Growth was evaluated at OD = 600 nm and MIC_{50} values were calculated by non-linear regression using Graphpad prism 7.

Genomic context of Rv0091.

MTAN in *E. coli* has been reported to be involved in SAH and MTA recycling and in quorum sensing pathways.[2] BT-DADMe-ImmA (**13**) inhibited production of the quorum sensing signaling molecule autoinducer (AI-2), but was not toxic to *E. coli* or *Vibrio cholera* growth, providing support for its role in quorum sensing.[1] Comparison of the gene maps for Rv0091

(NCBI gene ID: 886953), EcMTAN (NCBI gene ID: 948542) and HpMTAN (NCBI gene ID: 900251) indicate no organized operon function. In *E. coli*, the open reading frame for MTAN is adjacent to *btuF*, expressing a periplasmic B_{12} binding protein and *dgt*, known to express a dGTP triphosphohydrolase (Figure S4). In *H. pylori*, the adjacent Hp0090 is a malonyl-CoA: acyl carrier protein transacylase. Near the Rv0091 locus in *M. tuberculosis*, a nearby open reading frame, Rv0089 shares 41% identity in amino acids 32 to 146 (of 197) with the *E. coli* BioC protein, a SAM-dependent malonyl-acyl carrier protein methyltransferase, an early step in biotin synthesis.[40] In *E. coli*, the BioC protein is expressed from the *bioC* gene within the *bioABFCD* operon.[41] Based on the local gene organization near Rv0091, no insight is provided to its biological function, supporting a role in removing the 5'-dAdo product from the 21 potential radical SAM proteins in *M. tuberculosis*.

Conclusions.

Transition state analogues resembling the geometry and charge of the transition state for hydrolysis of 5'-dAdo by Rv0091 were synthesized and found to bind with pM to nM dissociation constants. The analogue that best captures the features of the preferred Rv0091 substrate 5'-dAdo and those containing different 5'-substituents were found to bind with pM to nM dissociation constants. (3*R*,4*S*)-3-Hydroxy-4-alkylpyrrolidine stereochemistry is preferred for these compounds, consistent with findings for related bacterial MTANs.[34] Comparison of 5'-alkylthio-DADMe-ImmA inhibitors that mimic the MTA substrate provided insight into the relative specificity for 5'-dAdo and 5'-methylthio adenosine substituents for Rv0091. Short-chain 5'-substituents are preferred for the 5'-deoxyalkyl-inhibitors while longer hydrophobic chains displayed tighter binding for the 5'-alkylthio-inhibitors. In both cases, substitution of polar atoms

into the 5'-substituent, i.e. CH_2- to O- reduces potency of the inhibitors. In silico docking of BT-DADMe-ImmA (**13**) and HT-DADMe-ImmA (**14**) with a model of Rv0091 showed similarity in binding to *E.coli* and *H. pylori* MTAN of the pyrrolidine and deazaadenine moieties, however differed at the 5'-alky or 5'-alkylthio groups. This difference is due to a methionine sterric clash near the 5'-substituent in the catalytic site of Rv0091. Isoleucine is present at this position in the MTANs from *E. coli* or *H. pylori*. Furthermore, weak antibacterial activity of these inhibitors against M*ycobacteria* indicates that Rv0091 functions in a non-essential pathway for growth.

SUPPORTING INFORMATION

Figure S1: Homology model of Rv0091 and superposition with HpMTAN and EcMTAN.

Figure S2: Comparison of primary sequence of Rv0091, HpMTAN and EcMTAN.

Figure S3: Superimposition of active site of HPMTAN and EcMTAN complex with BT-DADMe-ImmA; with Rv0091 modeled with BT-DADMe-ImmA and HT-DADMe-ImmA.

Figure S4: Analysis of neighboring genes of Rv0091, HpMTAN and EcMTAN.

AUTHOR INFORMATION

Correspondence author

*To whom correspondence should be addressed: vern.schramm@einstein.yu.edu

Author contributions

HAN and VLS designed inhibitors. GBE and PCT designed and performed the chemical synthesis of compounds. HAN designed and performed inhibitor experiments. RKH performed

molecular modeling and docking. VLS and HAN analyzed data. All authors contributed to writing the manuscript.

ACKNOWLEDGEMENTS

We acknowledge Drs. Scott Cameron (Einstein) for valuable discussions and A. Malek (Einstein) for help with the disc-diffusion assays. *M. smegmatis* mc^2155 and *M. tuberculosis* mc^26230 strains were gifts from the laboratory of Dr. William Jacobs (Einstein).

NOTES

Authors declare no conflict of interest with the contents in this article.

ABBREVIATIONS

5′-methylthioadenosine/*S*-adenosylhomocysteine nucleosidases (MTANs), 5′-methylthioadenosine (MTA), *S*-adenosylhomocysteine (SAH), 5′-deoxyadenosine (5′-dAdo), polyethelene glycol (PEG), *S*-adenosylmethionine (SAM), Kinetic isotope effect (KIE)

FUNDING

This work was supported by NIH research grant GM041916 and by the Michael Price Family Foundation.

REFERENCES

(1) Gutierrez, J. A., Crowder, T., Rinaldo-Matthis, A., Ho, M. C., Almo, S. C., and Schramm, V. L. (2009) Transition state analogs of 5'-methylthioadenosine nucleosidase disrupt quorum sensing. *Nat. Chem. Biol. 5*, 251-257.

(2) Parveen, N., and Cornell, K. A. (2011) Methylthioadenosine/S-adenosylhomocysteine nucleosidase, a critical enzyme for bacterial metabolism. *Mol. Microbiol. 79*, 7-20.

(3) Choi-Rhee, E., and Cronan, J. E. (2005) A nucleosidase required for in vivo function of the S-adenosyl-L-methionine radical enzyme, biotin synthase. *Chem. Biol. 12*, 589-593.

(4) Namanja-Magliano, H. A., Stratton, C. F., and Schramm, V. L. (2016) Transition state structure and inhibition of Rv0091, a 5'-deoxyadenosine/5'-methylthioadenosine nucleosidase from *Mycobacterium tuberculosis*. *ACS Chem. Biol. 11*, 1669-1676.

(5) Wang, J., Woldring, R. P., Roman-Melendez, G. D., McClain, A. M., Alzua, B. R., and Marsh, E. N. (2014) Recent advances in radical SAM enzymology: new structures and mechanisms. *ACS Chem. Biol. 9*, 1929-1938.

(6) Akiva, E., Brown, S., Almonacid, D. E., Barber, A. E., 2nd, Custer, A. F., Hicks, M. A., Huang, C. C., Lauck, F., Mashiyama, S. T., Meng, E. C., Mischel, D., Morris, J. H., Ojha, S., Schnoes, A. M., Stryke, D., Yunes, J. M., Ferrin, T. E., Holliday, G. L., and Babbitt, P. C. (2014) The structure-function linkage database. *Nucleic Acids Res. 42*, D521-530.

(7) McBryde, E. S., Meehan, M. T., Doan, T. N., Ragonnet, R., Marais, B. J., Guernier, V., Trauer, J. M. (2017) The risk of global epidemic replacement with drug-resistant Mycobacterium tuberculosis strains. *Int. J. Infect. Dis. 56*, 14-20.

(8) 15) Wolfenden, R. (1976) Transition state analog inhibitors and enzyme catalysis. *Annu. Rev. Biophys. Bioeng. 5*, 271-306.

(9) Wolfenden, R. (1969) Transition state analogues for enzyme catalysis. *Nature 223*, 704-705.

(10) Wolfenden, R., and Snider, M. J. (2001) The depth of chemical time and the power of enzymes as catalysts. *Acc. Chem. Res. 34*, 938-945.

(11) Schramm, V. L. (2007) Enzymatic transition state theory and transition state analogue design. *J. Biol. Chem. 282*, 28297-28300.

(12) Schramm, V. L. (1998) Enzymatic transition states and transition state analog design. *Annu. Rev. Biochem. 67*, 693-720.

(13) Schramm, V. L. (1999) Enzymatic transition-state analysis and transition-state analogs. *Methods Enzymol. 308*, 301-355.

(14) Singh, V., Lee, J. E., Nunez, S., Howell, P. L., and Schramm, V. L. (2005) Transition state structure of 5 '-methylthioadenosine/S-adenosylhomocysteine nucleosidase from *Escherichia coli* and its similarity to transition state analogues. *Biochemistry 44*, 11647-11659.

(15) Singh, V., and Schramm, V. L. (2007) Transition-state analysis of *S. pneumoniae* 5'-methylthioadenosine nucleosidase. *J. Am. Chem. Soc. 129*, 2783-2795.

(16) Gutierrez, J. A., Luo, M., Singh, V., Li, L., Brown, R. L., Norris, G. E., Evans, G. B., Furneaux, R. H., Tyler, P. C., Painter, G. F., Lenz, D. H., and Schramm, V. L. (2007) Picomolar inhibitors as transition-state probes of 5'-methylthioadenosine nucleosidases. *ACS Chem. Biol. 2*, 725-734.

(17) Wang, S., Cameron, S. A., Clinch, K., Evans, G. B., Wu, Z., Schramm, V. L., and Tyler, P. C. (2015) New Antibiotic Candidates against *Helicobacter pylori*. *J. Am. Chem. Soc. 137*, 14275-14280.

(18) Dairi, T. (2009) An alternative menaquinone biosynthetic pathway operating in microorganisms: an attractive target for drug discovery to pathogenic *Helicobacter* and *Chlamydia* strains. *J. Antibiot. (Tokyo) 62*, 347-352.

(19) Longshaw, A. I., Adanitsch, F., Gutierrez, J. A., Evans, G. B., Tyler, P. C., and Schramm, V. I. (2010) Design and synthesis of potent "sulfur-free" transition state analogue inhibitors of 5 '-methylthioadenosine nucleosidase and 5 '-methylthioadenosine phosphorylase. *J. Med. Chem. 53*, 6730-6746.

(20) Singh, V., Evans, G. B., Lenz, D. H., Mason, J. M., Clinch, K., Mee, S., Painter, G. F., Tyler, P. C., Furneaux, R. H., Lee, J. E., Howell, P. L., and Schramm, V. L. (2005) Femtomolar transition state analogue inhibitors of 5'-methylthioadenosine/S-adenosylhomocysteine nucleosidase from *Escherichia coli*. *J. Biol. Chem. 280*, 18265-18273.

(21) Haapalainen, A. M., Thomas, K., Tyler, P. C., Evans, G. B., Almo, S. C., and Schramm, V. L. (2013) *Salmonella enterica* MTAN at 1.36 angstrom resolution: a structure-based design of tailored transition state analogs. *Structure 21*, 963-974.

(22) Singh, V., Evans, G. B., Furneaux, R. H., Tyler, P. C., and Schramm, V. L. (2003) Targeting polyamine biosynthesis: Transition state of 5'-deoxy-5'-methylthioadenosine phosphorylase (MTAP) and transition state analogue inhibitors. *Biochemistry 42*, 8625-8625.

(23) Evans, G.B., Cameron, S.A., Luxenburger, A., Guan, R., Suarez, J., Thomas, K., Schramm, V. L., and Tyler, P. C. (2015) Tight binding enantiomers of pre-clinical drug candidates. *Biorg. Med. Chem, 23,* 5326-5333.

(24) Thomas, K., Cameron, S. A., Almo, S. C., Burgos, E. S., Gulab, S. A., and Schramm, V. L. (2015) Active site and remote contributions to catalysis in methylthioadenosine nucleosidases. *Biochemistry 54*, 2520-2529.

(25) Morrison, J. F., and Walsh, C. T. (1988) The behavior and significance of slow-binding enzyme inhibitors. *Adv. Enzymol. Relat. Areas Mol. Biol. 61*, 201-301.

(26) Larsen, M. H., Biermann, K., and Jacobs, W. R., Jr. (2007) Laboratory maintenance of *Mycobacterium tuberculosis*. *Curr. Protoc. Microbiol. Chapter 10*, Unit 10A 11.

(27) Sambandamurthy, V. K., Wang, X., Chen, B., Russell, R. G., Derrick, S., Collins, F. M., Morris, S. L., and Jacobs, W. R., Jr. (2002) A pantothenate auxotroph of *Mycobacterium tuberculosis* is highly attenuated and protects mice against tuberculosis. *Nat. Med. 8*, 1171-1174.

(28) Roy, A., Kucukural, A., and Zhang, Y. (2010) I-TASSER: a unified platform for automated protein structure and function prediction. *Nat. Protoc. 5*, 725-738.

(29) Emsley, P., and Cowtan, K. (2004) Coot: model-building tools for molecular graphics. *Acta Crystallogr. D Biol. Crystallogr. 60*, 2126-2132.

(30) Trott, O., and Olson, A. J. (2010) AutoDock Vina: improving the speed and accuracy of docking with a new scoring function, efficient optimization, and multithreading. *J. Comput. Chem. 31*, 455-461.

(31) Adams, P. D., Afonine, P. V., Bunkoczi, G., Chen, V. B., Davis, I. W., Echols, N., Headd, J. J., Hung, L. W., Kapral, G. J., Grosse-Kunstleve, R. W., McCoy, A. J., Moriarty, N. W., Oeffner, R., Read, R. J., Richardson, D. C., Richardson, J. S., Terwilliger, T. C., Zwart, P. H. (2010) PHENIX: a comprehensive Python-based system for macromolecular structure solution. *Acta Crystallogr. D Biol. Crystallogr. 66*, 213–221.

(32) Wang, S., Haapalainen, A. M., Yan, F., Du, Q., Tyler, P. C., Evans, G. B., Rinaldo-Matthis, A., Brown, R. L., Norris, G. E., Almo, S. C., and Schramm, V. L. (2012) A picomolar transition state analogue inhibitor of MTAN as a specific antibiotic for *Helicobacter pylori*. *Biochemistry 51*, 6892-6894.

(33) Singh, V., Luo, M., Brown, R. L., Norris, G. E., and Schramm, V. L. (2007) Transition-state structure of *Neisseria meningitides* 5'-methylthioadenosine/S-adenosylhomocysteine nucleosidase. *J. Am. Chem. Soc. 129*, 13831-13833.

(34) Evans, G. B., Cameron, S. A., Luxenburger, A., Guan, R., Suarez, J., Thomas, K., Schramm, V. L., and Tyler, P. C. (2015) Tight binding enantiomers of pre-clinical drug candidates. *Bioorg. Med. Chem. 23*, 5326-5333.

(35) Lee, J. E., Singh, V., Evans, G. B., Tyler, P. C., Furneaux, R. H., Cornell, K. A., Riscoe, M. K., Schramm, V. L., and Howell, P. L. (2005) Structural rationale for the affinity of pico- and femtomolar transition state analogues of *Escherichia coli* 5'-methylthioadenosine/S-adenosylhomocysteine nucleosidase. *J. Biol. Chem. 280*, 18274-18282.

(36) Singh, V., Shi, W., Almo, S. C., Evans, G. B., Furneaux, R. H., Tyler, P. C., Painter, G. F., Lenz, D. H., Mee, S., Zheng, R., and Schramm, V. L. (2006) Structure and inhibition of a quorum sensing target from *Streptococcus pneumoniae*. *Biochemistry-Us 45*, 12929-12941.

(37) Shiloh, M. U., and Champion, P. A. (2010) To catch a killer. What can mycobacterial models teach us about *Mycobacterium tuberculosis* pathogenesis? *Curr. Opin. Microbiol. 13*, 86-92.

(38) Sassetti, C. M.,and Rubin, E. J. (2003) Genetic requirements for mycobacterial survival during infection. Proc. Nat. Acad. Sci. U. S. A. *100*, 12989-12994.

(39) Griffin, J. E., Gawronski, J. D., Dejesus, M. A., Ioerger, T. R., Akerley, B. J., and Sassetti, C.M. (2011) High-resolution phenotypic profiling defines genes essential for mycobacterial growth and cholesterol catabolism. *PLoS. Pathog. 7*(9):e1002251.

(40) Lin, S., and Cronan, J. E. (2012) The BioC O-methyltransferase catalyzes methyl esterification of malonyl-acyl carrier protein, an essential step in biotin synthesis. *J. Biol. Chem 287*, 37010-37020.

(41) Cao, X., Zhu, L., Hu, Z., and Cronan, J. E. (2017) Expression and activity of the BioH esterase of biotin synthesis is independent of genome context. *Nature Sci. Reports 7*, 2141

For table of contents use:

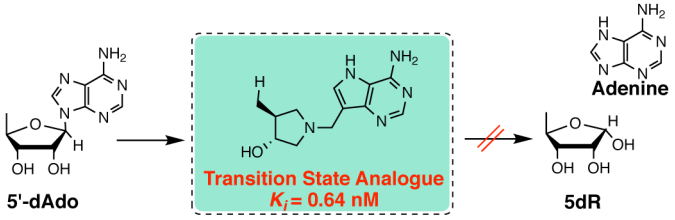

For table of contents use: